

# NUMERICAL SIMULATION OF EMITTER AND BASE DOPING EFFECTS IN SILICON SOLAR CELLS USING A ONE-DIMENSIONAL MODEL

Nur Zarifah Zulkifle<sup>1</sup>, Madhiyah Yahaya Bermakai<sup>1\*</sup>, Mohd Zaki Mohd Yusoff<sup>2</sup>, Noorsyam Yusof<sup>1</sup>

<sup>1</sup>Department of Physics, Faculty of Applied Sciences, Universiti Teknologi MARA (UiTM), Cawangan Perlis, Kampus Arau, 02600 Arau, Perlis, Malaysia

<sup>2</sup>School of Physics and Material Studies, Faculty of Applied Sciences, Universiti Teknologi MARA (UiTM) Shah Alam, 40450 Shah Alam, Selangor, Malaysia

\*Corresponding author: madhiyah@uitm.edu.my

#### **Abstract**

Doping concentration plays a crucial role in determining the electrical and photovoltaic performance of crystalline silicon solar cells. However, the optimum combination of emitter and base doping remains debated due to trade-offs between conductivity, recombination, and efficiency. In this study, one-dimensional simulations using PC1D were carried out to systematically vary the emitter and base doping concentrations across realistic ranges. The results show that the highest efficiency of 13.5% is achieved with an emitter doping concentration of  $1x10^{18}$  cm<sup>-3</sup> and base doping concentration of 3-4 x  $10^{19}$  cm<sup>-3</sup>. This work highlights how balancing doping levels between emitter and base layers can mitigate recombination losses while maintaining conductivity, providing design guidance for optimizing silicon solar cell efficiency.

Keywords: photovoltaic, silicon, solar cell, dopant density, PC1D

Article History:- Received: 19 June 2025; Revised: 5 October 2025; Accepted: 10 October 2025; Published: 31 October 2025 © by Universiti Teknologi MARA, Cawangan Negeri Sembilan, 2025, e-ISSN: 2289-6368 DOI: 10.24191/joa.v13i2.7041

### Introduction

Solar cells are a critical renewable energy technology, with crystalline silicon (c-Si) devices continuing to dominate the photovoltaic (PV) market due to their high efficiency, material abundance, and technology maturity (Chiras, 2016; Maka & Alabid, 2022). Despite these advantages, the efficiency of crystalline silicon (c-Si) solar cells remains limited by optical losses and electrical recombination, constraining further performance gains.

The photovoltaic conversion efficiency of solar cells improvement has been one of the topics that are constantly discussed in the photovoltaic field. There are two techniques that are effective to increase the efficiency of the photovoltaic conversion which are enhance absorption of incident sunlight on the silicon surface by reducing the reflection loss or improve the photovoltaic effect by reducing the electrical loss (Andreani et al., 2019; Sultan et al., 2023). Solar cells consist of two primary layers: a thin upper layer, known as the n-type layer, and a thicker lower layer, referred to as the p-type layer, as illustrated in Figure 1. Among electrical factors, doping concentration in the emitter (n-type) and base (p-type) layers plays a decisive role in device performance (Bult et al., 2013; Lüssem et al., 2013). Doping directly influences the open-circuit voltage ( $V_{\rm OC}$ ), short-circuit current ( $I_{\rm SC}$ ), and overall efficiency of the solar cell. A heavily doped emitter enhances conductivity and reduces series resistance, which can improve current collection, but excessive doping increases recombination at the junction, reducing  $V_{\rm OC}$  and efficiency. Conversely, a lightly doped base widens the depletion region and enhances carrier lifetime, improving  $V_{\rm OC}$ , but too low a doping level can reduce conductivity and lower  $I_{\rm SC}$ . Thus, the trade-off between conductivity and recombination at different doping levels is central to optimizing silicon solar cells.



Several studies have investigated this trade-off. Subramanian et al. (2022) reported the importance of emitter doping optimization for c-Si solar cells, while Thirunavukkarasi et al. (2021) highlighted the sensitivity of device performance to base doping levels is equally critical in determining  $V_{\rm OC}$ ,  $I_{\rm SC}$ , and fill factors. Nevertheless, the optimal balance between emitter and base doping concentrations across practical ranges remains unclear. This study aims to numerically analyze the influence of emitter and base doping concentrations on c-Si solar cell performance using the PC1D one-dimensional simulation tool. By systematically varying the doping levels within realistic ranges, the conditions that maximize efficiency will be identified and provide guidance for future device design in silicon solar cell technologies.

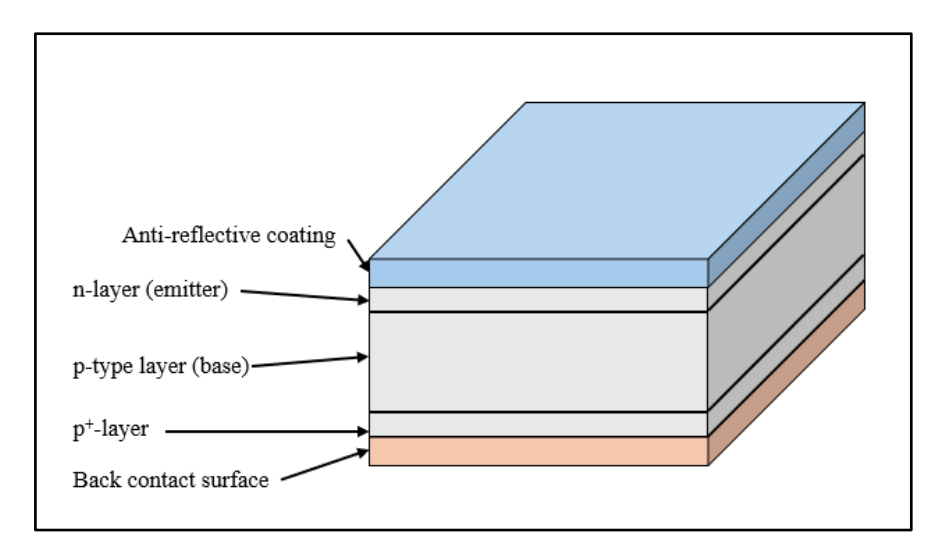


Figure 1. Basic solar cell structure

# Methods

In this study, the PC1D simulation software was employed to design and analyze the performance of crystalline silicon solar cells. PC1D is a widely validated one-dimensional numerical tool that efficiently solves carrier transport and recombination equations, allowing detailed analysis of electrical characteristics without complex fabrication steps. This makes it particularly suitable for exploring the effects of emitter and base doping concentration prior to experimental implementation. The experimental setup is summarized in Table 1. The device area was set to 250.0 cm², representing a standard cell dimension commonly reported in PC1D simulations (Subramanian et al., 2022). Both the front and rear surfaces textured to a depth of 3  $\mu$ m and an angle of 54.74°, corresponding to the typical anisotropic etching geometry of (100)-oriented c-Si wafers. This configuration enhances light trapping while maintaining consistency with industrially relevant designs.

The thickness of the wafer was fixed at 180  $\mu$ m, which is within the range of commercial monocrystalline silicon wafers and allows for balancing mechanical stability with photon absorption depth. The intrinsic carrier concentration ( $1x10^{10}$  cm.3 at 300K), surface recombination velocities (10,000 cm/s), and bulk lifetime (100  $\mu$ s) were chosen based on literature values to provide realistic recombination conditions (Thirunavukkarasu et al., 2021). The front and rear surface coatings were set to zero thickness with refractive index 1, to specifically isolate the effect of doping concentration without interference from anti-reflective coatings. The excitation file "one-sun.exc" was used as the excitation mode, as it provides key photovoltaic parameters ( $I_{SC}$ ,  $V_{OC}$ ,  $P_{max}$ ), while "scan-qe.exc" was not adopted since this study focuses on efficiency rather than quantum efficiency analysis (Belarbi et al., 2014).

For the doping study, emitter concentrations were varied from  $1\times10^{17}$  cm<sup>-3</sup> to  $1\times10^{21}$  cm<sup>-3</sup>, consistent with reported ranges for phosphorus-doped n<sup>+</sup> emitters in c-Si solar cells (Andreani at al., 2019). The



optimum emitter value was then fixed to investigate base doping concentrations, which were varied between  $3\times10^{16}$  cm<sup>-3</sup> to  $3\times10^{20}$  cm<sup>-3</sup>, representing boron doping levels for p-type substrates in both lightly and heavily doped regimes. These wide parameter ranges were selected to cover both moderate and heavy doping scenarios, ensuring that the trade-offs between conductivity, recombination, and depletion width could be fully evaluated. The spectrum used in the simulation is AM1.5G, as recommended by Bremner et al., 2008. A schematic workflow of the simulation process is illustrated in Figure 2, outlining the key stages of the study. The workflow begins with the input of baseline device parameters, followed by the systematic variation of emitter and base doping concentrations, and concludes with the extraction and analysis of output parameters.

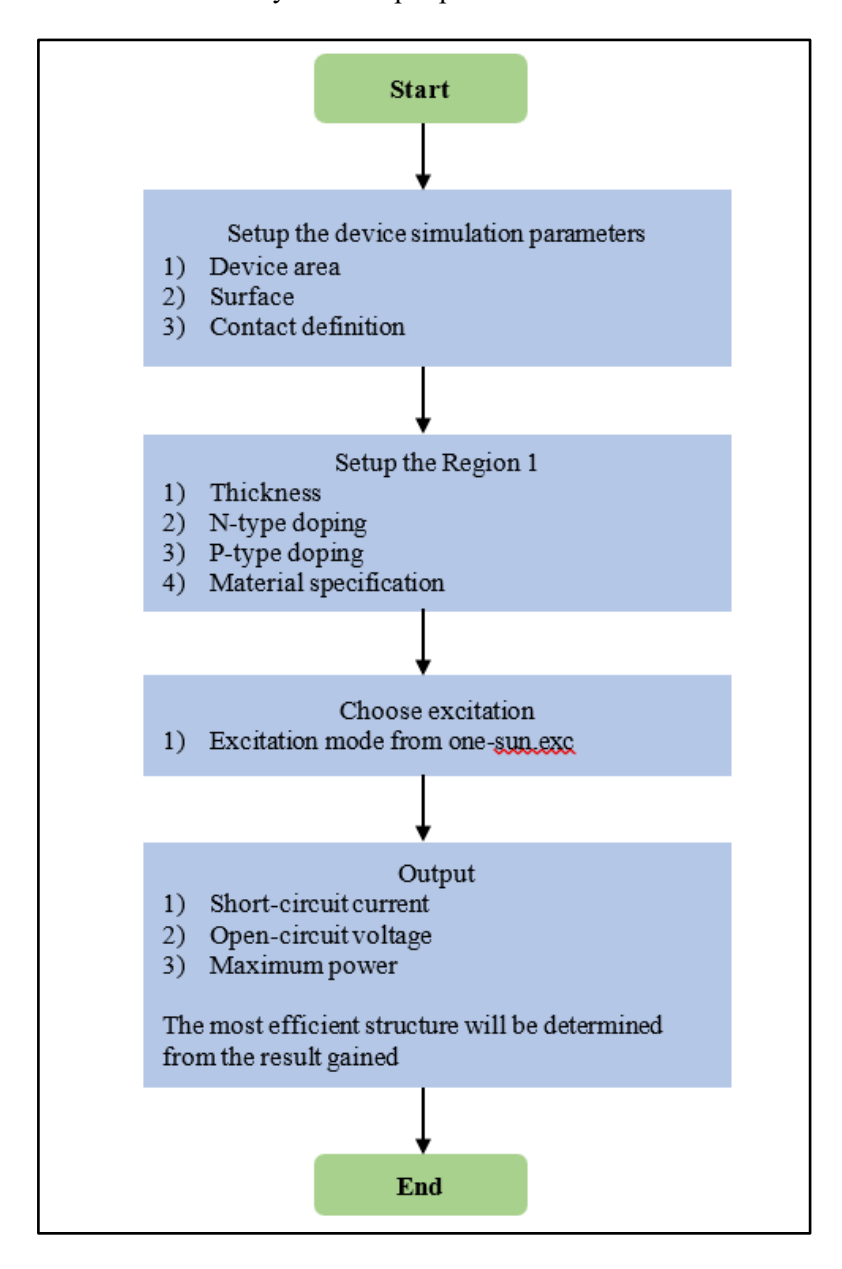


Figure 2. Simulation workflow of the simulation process.

During the simulation, the transient or steady-state convergence failures were observed at extremely high doping level ( $>10^{20}$  cm<sup>-3</sup>). These failures arise because the very high carrier concentrations produce numerical instability and physically unrealistic junction profiles, where Auger recombination dominates and the quasi-neutral region becomes negligible. Such results indicate the non-physical limits of heavy doping rather than computational errors and thus help define the upper practical boundary for emitter and base doping concentrations.



It is important to note that while PC1D provides accurate carrier transport modeling in one dimension, it neglects certain practical effects such as metal shading, busbar resistance, and advanced surface passivation. As a result, the simulated efficiencies are expected to be slightly lower than those of commercial solar cells, but the relative performance trends and optimized doping levels remain valid and informative.

Table 1. Control parameters for simulation (Subramanian et al., 2022).

Parameters	Values		
Device area	$250.0 \text{ cm}^2$		
Front surface texture depth	54.74°/3 μm		
Rear surface texture depth	-		
Front/rear surface coating	-		
Internal optical reflectance	Enabled		
Thickness	180 μm		
Intrinsic concentration at 300K	$1 \times 10^{10}  \text{cm}^{-3}$		
n <sup>+</sup> diffusion	$1 \times 10^{20}  \text{cm}^{-3}$		
p <sup>+</sup> diffusion	$3x10^{18}  \text{cm}^{-3}$		
Front and rear SRV	10000  cm/s		
Bulk recombination	100 μs		
Temperature	25 °C		

### **Results and Discussion**

# **Emitter doping effect**

Figure 3 and Table 2 show the current-voltage (I-V) characteristics and efficiency trends for different emitter doping concentrations. From the result gained, the efficiency of the solar cell based on the various values of emitter doping were calculated. The formula stated in Equation (1) is used to calculate the efficiency (Goodnick & Honsberg, 2022).

$$efficiency, \eta = \frac{P_{max}}{E \times A_c} \tag{1}$$

Where,

E = incident radiation flux

 $A_c$  = Area of collector

As the emitter doping level increases from  $1 \times 10^{17}$  cm<sup>-3</sup> to  $1 \times 10^{18}$  cm<sup>-3</sup>, the efficiency improves from 13.1% to 13.4%. This enhancement arises from reduced series resistance and improved electron transport across the junction. Moderate doping increases the majority carrier concentration in the emitter, improving conductivity and facilitating charge separation, which directly enhances the short-circuit current ( $I_{SC}$ ) and fill factor.

However, when the doping concentration exceeds 1 x 10<sup>19</sup> cm<sup>-3</sup>, the efficiency begins to decrease sharply (from 13.2% down to 7.1%). This degradation can be explained by increased Auger recombination, a process in which excess free carriers interact such that the energy released during electron-hole recombination is transferred to third carrier rather than emitted as a photon. High doping introduces a large concentration of free carriers (electrons in the n<sup>+</sup> emitter), raising the probability of these three-body interactions. Consequently, the minority carrier lifetime drops significantly, limiting the number of photogenerated carriers that can be collected before recombination.

Additionally, Shockley-Read-Hall (SRH) recombination at defect sites becomes more pronounced under heavy doping, further reducing the open-circuit voltage ( $V_{OC}$ ). These effects combine to produce the observed decline in efficiency. The result aligns well with the observation Subramanian et al. (2022) and Guerra et al. (2018), who both reported the emitter doping near  $10^{18}$  cm<sup>-3</sup> achieves an optimal



balance between conductivity and recombination in crystalline silicon solar cells. Thus, the emitter doping concentration of  $1x10^{18}$  cm<sup>-3</sup> offers the best trade-off – minimizing resistive losses while maintaining a sufficiently long carrier lifetime for efficient collection.

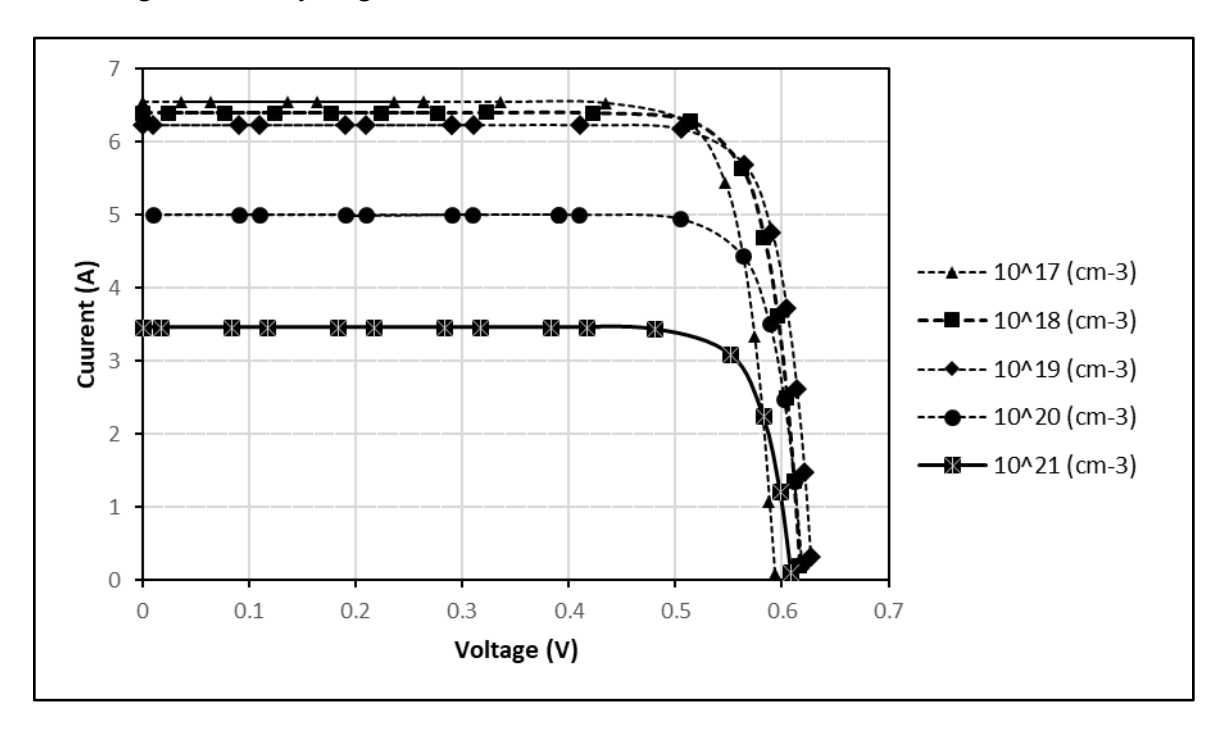


Figure 3. Current-Voltage characteristic of the emitter layer doping concentration.

Table 2. The efficiency of solar cells due to doping at emitter layer.

Emitter Doping	Short circuit, I <sub>SC</sub> (amps)	Open circuit, Voc (volts)	Max base power, P <sub>Max</sub> (watts)	Efficiency, η (%)	
1x10 <sup>17</sup>	-6.552	0.5925	3.207	13.1%	
$1x10^{18}$	-6.393	0.6173	3.272	13.4%	
$1x10^{19}$	-6.230	0.6279	3.233	13.2%	
$1x10^{20}$	-5.004	0.6198	2.553	10.4%	
$1x10^{21}$	-3.458	0.6098	1.737	7.1%	
$1x10^{22}$	Transient Convergence Failure				
$1x10^{23}$	Transient Convergence Failure				

# **Base doping effect**

The influence of base doping concentration on the I-V characteristics is shown in Figure 4 and summarized in Table 3. Efficiency improves with increasing base doping up to approximately 3-4 x  $10^{19}$  cm<sup>-3</sup>, where a maximum of 13.54% is achieved. At low doping levels (3 x  $10^{16}$  – 3 x  $10^{17}$  cm<sup>-3</sup>), the base has a wide depletion region that supports better separation of photogenerated carriers but suffers from increased resistive losses due to poor conductivity. This results in a slightly reduce  $I_{SC}$  and fill factor.

As the base doping increases, the improved conductivity and reduced resistive loss enhance  $I_{SC}$  and fill factor. However, when doping exceeds  $10^{20}$  cm<sub>-3</sub>, Auger recombination within the base becomes dominant, reducing the minority carrier lifetime and flattening the potential barrier at the junction. Excessive base doping also narrows the depletion region, limiting charge collection from deeper regions of the cell. The observed convergence failures in simulation at very high doping levels (>  $10^{20}$  cm<sup>-3</sup>) are consistent with physical expectations, as extreme impurity concentrations distort the p-n junction profile.

This trade-off between conductivity and recombination reflects the fundamental physical constraint of



silicon solar cell: increasing carrier density inevitably increases recombination probability. The optimized base doping range of  $3-4 \times 10^{19}$  cm<sup>-3</sup> observed here corresponds to the point where improved electrical conduction balances recombination-induced carrier loss. These findings are consistent with prior simulation studies by Thirunavukkarasu et al. (2021) and Andreani et al. (2019), indicating that optimal base doping typically lies in the  $10^{19}$  cm<sup>-3</sup> range.

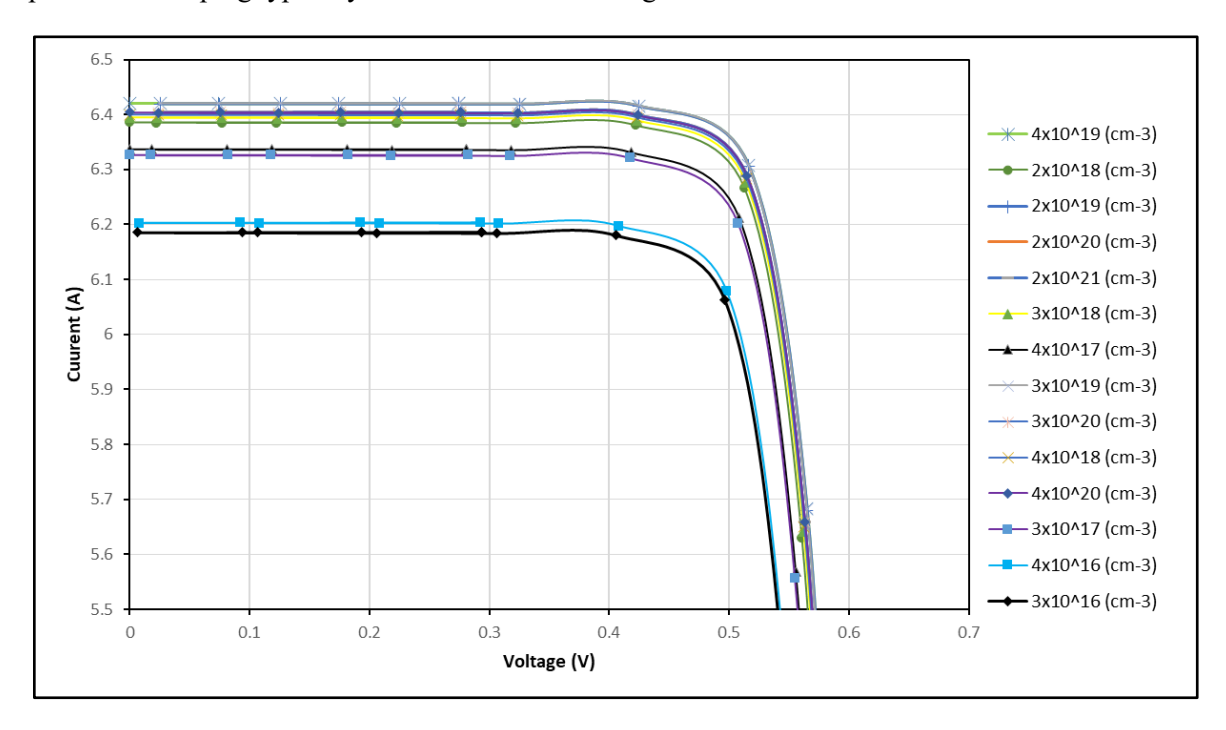


Figure 4. Current-Voltage characteristic of base layer doping concentration.

Table 3. The efficiency of solar cell due to doping at base layer.

Base doping	Short circuit, Isc	Open circuit, Voc	Max base power, Pmax	Efficiency, η (%)	
$3x10^{16}$	-6.1.86	0.5977	3.052	12.49	
$3x10^{17}$	-6.326	0.6093	3.191	13.06	
$3x10^{18}$	-6.393	0.6173	3.272	13.39	
$3x10^{19}$	-6.420	0.6213	3.308	13.54	
$3x10^{20}$	-6.404	0.6189	3.286	13.45	
$3x10^{21}$	Transient Convergence Failure				
$2x10^{18}$	-6.384	0.6161	3.260	13.34	
$2x10^{19}$	-6.419	0.6211	3.306	13.53	
$2x10^{20}$	-6.405	0.6190	3.287	13.45	
$2x10^{21}$	-6.404	0.6190	3.286	13.45	
$2x10^{22}$	Steady-State Convergence Failure				
$4x10^{16}$	-6.203	0.5989	3.068	12.56	
$4x10^{17}$	-6.336	0.6104	3.203	13.11	
$4x10^{18}$	-6.399	0.6181	3.279	13.42	
$4x10^{19}$	-6.420	0.6213	3.308	13.54	
$4x10^{20}$	-6.404	0.6189	3.286	13.45	
$4x10^{21}$	Transient Convergence Failure				

# **Comparative Analysis and Physical Insights**

The doping profiles are often optimized to reduce recombination at the surface and at the junction. Lightly doped emitter layers are used to reduce surface recombination, while the base layer is typically heavily doped to improve conductivity and reduce series resistance. The recombination rate, which is inversely related to the carrier lifetime, is influenced by doping concentration. High doping concentrations can lead to Auger recombination and Shockley-Read-Hall recombination, both of which



reduce the cell's efficiency by increasing the rate at which charge carriers recombine before contributing to the current. The doping concentration should be carefully optimized for maximum solar cell efficiency, balancing factors such as current generation, voltage, recombination rates, and the width of the depletion region.

The results from both emitter and base optimization studies reveal complementary effects. An optimum balance – emitter 1 x  $10^{18}$  cm<sup>-3</sup> and base 3-4 x  $10^{19}$  cm<sup>-3</sup> – yields the maximum efficiency of 13.5%. compared to previous simulation studies (Subramanian et al., 2022); Thirunavukkarasu et al., 2021), the optimum doping values in this work are slightly higher, which may be attributed to difference in assumed wafer thickness (180  $\mu$ m in this study) and surface recombination velocities. Thicker wafer benefits from slightly higher base doping to maintain conductivity and minimize recombination within the diffusion length.

The observed decline in efficiency at extreme doping levels reflects the Auger recombination mechanism, where the recombination rate increases approximately with the cube of carrier concentration (R  $\alpha$  n<sup>3</sup> or p<sup>3</sup>). As doping rises, carrier lifetimes shorten dramatically, leading to lower  $V_{OC}$  and  $I_{SC}$ . This explains why, even though conductivity improves with heavy doping, the overall efficiency declines. The maximum simulated efficiency of 13.5%, though lower than typical industrial c-Si solar cells (15 – 23%), can be rationalized by the simplified cell structure used in the simulation. In this work, no anti-reflective coating (ARC), no front or rear passivation layers, and no metal shading or busbar losses were modeled. These simplifications were intentional to isolate the electrical effects of doping, and advanced passivation techniques that reduce optical and surface recombination losses, thereby boosting efficiency.

Therefore, while the absolute efficiency values are lower than industrial benchmarks, the relative trends and optimum doping levels remain valid, offering meaningful insight into the fundamental doping-recombination trade-offs in silicon solar cells. The present results also provide guidance for future simulations that can incorporate optical effects and surface passivation to further approach experimental efficiencies.

# Conclusion

This study employed one-dimensional PC1D simulations to analyze how emitter and base doping concentrations affect the performance of crystalline silicon solar cells. The results confirm that doping levels critically influence key photovoltaics parameters – open-circuit voltage ( $V_{\rm OC}$ ), short-circuit current ( $I_{\rm SC}$ ), and overall efficiency – through their effects on carrier recombination and conductivity. The optimum configuration was obtained with an emitter doping concentration of 1 x 10<sup>18</sup> cm<sup>-3</sup> and a base doping concentration between 3 x 10<sup>19</sup> cm<sup>-3</sup> and 4 x 10<sup>19</sup> cm<sup>-3</sup>, producing a maximum simulated efficiency of 13.5%. While this efficiency is lower than that of commercial cells, the simplified structure (without ant-reflective coatings or advanced passive action) isolates the pure electrical effects of doping, providing valuable design insight.

Importantly, this study demonstrates that careful balancing of emitter and base doping can significantly improve device modeling accuracy and guide fabrication strategies aimed at minimizing recombination losses. The results offer a quantitative framework for understanding the doping-recombination traded-off, supporting further optimization of silicon solar cells. Future work should integrate optical enhancements such as anti-reflective coatings and surface texturing, as well as explore graded or selective doping profiles, to extend these insights toward practical high-efficiency solar designs.

## Acknowledgement/Funding

Authors would like to thank Faculty of Applied Sciences, Universiti Teknologi MARA (UiTM), Perlis Branch, Malaysia. The authors received no financial support for the research.

### **Author Contribution**

NZ Zulkifle – data curation, writing – original draft; M Yahaya Bermakai – conceptualization, data curation, writing – editing. N Yusof – Reviewing & evaluation; MZ Mohd Yusoff – supervision.



#### **Conflict of Interest**

Authors declare no conflict of interest.

### Declaration on the Use of Generative AI

The authors acknowledge the use of artificial intelligence (AI) tools in the preparation of this manuscript. Specifically, ChatGPT (OpenAI) was used to assist with language refinement, idea clarification, and sentence structuring, while Grammarly was employed for grammar checking. All content generated or suggested by these tools was critically reviewed and revised by the authors to ensure accuracy, originality and academic integrity.

### References

Andreani, L. C., Bozzola, A., Kowalczewski, P., Liscidini, M., & Redorici, L. (2019). Silicon solar cells: toward the efficiency limits. *Advances in Physics: X*, 4(1), 1548305. https://doi.org/10.1080/23746149.2018.1548305

Belarbi, M., Benyoucef, A., & Benyoucef, B. (2014). Simulation of the solar cells with pc1d, application to cells based on silicon. *Advanced Energy: An International Journal* 1(3).

Bremner, S. P., Levy, M. Y., & Honsberg, C. B. (2008). Analysis of tandem solar cell efficiencies under AM1.5G spectrum using a rapid flux calculation method. *Progress in Photovoltaics: Research and Applications*, 16(3), 225–233. https://doi.org/10.1002/PIP.799

Bult, J. B., Crisp, R., Perkins, C. L., & Blackburn, J. L. (2013). Role of dopants in long-range charge carrier transport for p-type and n-type graphene transparent conducting thin films. *ACS nano*, 7(8), 7251-7261.

Chiras, D. D. (2016). Power from the Sun. In *Achieving Energy Independence*. Gabriola Island, Canada: New Society Publishers.: pp. 43-64.

Guerra, N., Guevara, M., Palacios, C., & Crupi, F. (2018). Operation and physics of photovoltaic solar cells: an overview. *I+D Tecnologico*, *14*(2), 84-95.

Goodnick, S. M., & Honsberg, C. (2022). Solar Cells. In *Springer Handbook of Semiconductor Devices*. Cham, Switzerland: Springer: pp. 699-745 https://doi.org/10.1007/978-3-030-79827-7 19

Lüssem, B., Riede, M., & Leo, K. (2013). Doping of organic semiconductors. *physica status solidi (a)*, 210(1), 9-43.

Maka, A. O. & Alabid, J. M. (2022). Solar energy technology and its roles in sustainable development. *Clean Energy*, 6(3), 476–483. https://doi.org/10.1093/CE/ZKAC023

Subramanian, M., Nagarajan, B., Ravichandran, A., Subhash Betageri, V., Thirunavukkarasu, G. S., Jamei, E., Seyedmahmoudian, M., Stojcevski, A., Mekhilef, S., & Minnam Reddy, V. R. (2022). Optimization of effective doping concentration of emitter for ideal c-Si solar cell device with PC1D simulation. *Crystals*, *12*(2), 244. https://doi.org/10.3390/CRYST12020244

Sultan, S. M., Tso, C. P., Ervina, E. M. N., & Abdullah, M. Z. (2023). A cost effective and economic method for assessing the performance of photovoltaic module enhancing techniques: Analytical and experimental study. *Solar Energy*, 254, 27-41.

Thirunavukkarasu, G. S., Seyedmahmoudian, M., Chandran, J., Stojcevski, A., Subramanian, M., Marnadu, R., Alfaify, S., & Shkir, M. (2021). Optimization of mono-crystalline silicon solar cell devices using PC1D simulation. *Energies*, *14*(16), 4986. https://doi.org/10.3390/EN14164986